Journal of Cultural Heritage 77 (2026) 96–108

Contents lists available at ScienceDirect

Journal of Cultural Heritage

journal homepage: www.elsevier.com/locate/culher

Original article

Biodeterioration aspects of the 16th century icon “Deesis tier of thirteen figures” by the fungus *Iodophanus* sp. STG-150: a range of materials for biodegradation and selection of target antiseptics

Daria A. Avdanina[a,*], Olga B. Vorobyova[c], Anna A. Ermolyuk[a], Nikolay P. Simonenko[d], Ivan A. Volkov[e], Liudmila A. Alexandrova[f], Maxim V. Jasko[f], Dmitry A. Makarov[f], Maxim A. Khomutov[f], Elena N. Khurs[f], Alexey R. Khomutov[f], Olga B. Riabova[b], Vadim A. Makarov[b], Egor V. Troyan[c], Michael V. Shitov[c], Alexander A. Zhgun[a]

[a] *Skryabin Institute of Bioengineering, Research Center of Biotechnology RAS, Moscow, Russia*
[b] *Bach Institute of Biochemistry, Research Center of Biotechnology RAS, Moscow, Russia*
[c] *State Tretyakov Gallery, Moscow, Russia*
[d] *Kurnakov Institute of General and Inorganic Chemistry RAS, Moscow, Russia*
[e] *Institute of Physics and Technology, Dolgoprudniy, Russia*
[f] *Engelhardt Institute of Molecular Biology, RAS, Moscow, Russia*

ARTICLE INFO

Article history:
Received 23 July 2025
Accepted 3 November 2025
Available online 20 November 2025

Keywords:
Biodeterioration
Fungi
Icons
Restoration
Art materials
H-phosphinic analogue of aspartate
Alkyl nucleosides
Iodophanus sp

ABSTRACT

Cultural heritage objects—particularly, paintings—consist of materials that can be deteriorated by specialized microorganisms. In this regard, it is imperative to both delineate their biodegradation capacity as well as select target antiseptics that can prevent this process, while remaining inert towards the painting materials. This study characterized the fungus *Iodophanus* sp. STG-150, belonging to the *Pezizaceae* family, which was isolated from bio-lesion sites of the 16th century painting “Deesis Tier of 13 Figures”—a unique habitat that has not been described before. To analyse their ability to degrade painting materials, cells of the STG-150 strain were inoculated onto crafted mock layers that were coloured with individual painting materials, including basis, adhesives, egg yolk emulsion and tempera paints, watercolour, and varnishes. STG-150 was able to actively grow on basis (pavoloka), adhesives (sturgeon glue and mordant), egg yolk emulsion, and ochre-pigment. Contrastingly, moderate growth was observed on watercolour black and varnishes (linseed oil, acrylic varnish). The addition of cobalt green, strontian yellow, cadmium red, and grey-green to the egg yolk resulted in significant antifungal resistance. Furthermore, the addition of zinc white and burnt sienna completely inhibited STG-150 growth. Using scanning electron microscopy (SEM), it was observed that STG-150 produced two morphological forms of mycelium on the egg yolk emulsion and ochre-pigment—vegetative and aerial with conidia. All other art materials revealed only vegetative mycelium. Fourier-transform infrared spectroscopy (FTIR) also detected areas of STG-150 growth at the periphery of the inoculation site that were invisible to the eye. Mineral pigments as an antiseptic cannot be used to protect paintings from biodegradation, as they introduce unwanted colouration and degrade the original colour. Consequently, a targeted selection of new generation antiseptics were developed for the protection of paintings against STG-150: (i) nucleoside derivatives: N^4-dodecyl-5-methyl-2′-deoxycytidine (Ala 54), N^4-dodecyl-5-methylcytidine (Ala 106), 3′-amino-N^4-dodecyl-5-methyl-2′,3′-dideoxycytidine (SOV4); (ii) sulphur-containing heterocyclic compounds: 3,5-dinitropyridin-2-yl thiocyanate – (M1), 4-nitro-2,1,3-benzothiadiazol-5-yl thiocyanate (M2), 3-cyano-5-nitropyridin-2-yl thiomorpholine-4-carbodithioate (M3), and ethyl 1–hydroxy-6-thioxo-1,6-dihydropyridine-3-carboxylate (M4); as well as (iii) *H*-phosphinic amino acid analogues: 1-

* Corresponding author.
E-mail addresses: d.avdanina@gmail.com (D.A. Avdanina), m.g.stepanov@gmail.com (O.B. Vorobyova), anya_ermolyuk@mail.ru (A.A. Ermolyuk), n_simonenko@mail.ru (N.P. Simonenko), volkov256@yandex.ru (I.A. Volkov), ala2004_07@mail.ru (L.A. Alexandrova), 2003_maxim@mail.ru (M.V. Jasko), dmitmakarov_97@mail.ru (D.A. Makarov), hommaximus@mail.ru (M.A. Khomutov), enkhurs@yandex.ru (E.N. Khurs), alexkhom@list.ru (A.R. Khomutov), o.riabova@fbras.ru (O.B. Riabova), makarov@inbi.ras.ru (V.A. Makarov), troianev@tretyakov.ru (E.V. Troyan), shitovmv@tretyakov.ru (M.V. Shitov), zzhgun@mail.ru (A.A. Zhgun).

https://doi.org/10.1016/j.culher.2025.11.001

Aminoethyl-*H*-phosphinic acid (Ala-pH), L-amino-2-methylpropyl-*H*-phosphinic acid (Val-pH), 1-amino-3-methylthiopropyl-*H*-phosphinic acid (Met-pH), and L-amino-2-carboxyethyl-*H*-phosphinic acid (Asp-α-pH). Their effects completely suppressed the growth of *Iodophanus* sp. STG-150. Further exploration of the antifungal activity and compatibility of these successful biocides with paints and varnishes should be undertaken in future studies on mock layers.

1. Introduction

Microorganisms occur ubiquitously in nature, under widely varying conditions and locations. They have successfully colonized a variety of objects, including works of art created with various organic and inorganic materials. Biodegradation can affect both monuments [1–4] and easel art [5–7] that are directly exposed to the air, as well as paper manuscripts, books [8,9], and even cinematographic films [10]. Several of the components in these artworks are suspected to be biodegradable—such as paper, wood, textile, and pigments dissolved in different binders [11]. The latter commonly include oil, egg yolk or gum arabic. Moreover, some artworks can be composed of soft, free-flowing materials such as pressed charcoal, sanguine, sepia, sauce, pastel. For preservation, artworks are usually coated with protective varnishes. However, despite this preventive measure, adverse temperature and humidity conditions or transportation to an exhibition may disrupt the maintenance regime for art objects, consequently leading to the development of mould fungi. Some fungal strains (*Penicillium, Aspergillus, Alternaria Aureobasidium, Cladosporium, Trichoderma*) [12,13] are known to colonise the pigment of artworks and produce myriad colours due to their secretions. Furthermore, fungi may secrete harmful substances, such as allergens, which may cause hypersensitivity to art conservators [14] and museum visitors. Even long-term conservation of heritage collections in museums maintained under suitable environmental conditions may not suffice.

This study focused on an ancient Russian icon "Deesis Tier of 13 Figures", measuring 215 x 59.5 cm (Fig. 1) The icon entered the State Tretyakov Gallery (STG) in the 1930s. The uniqueness of the icon lies in the arrangement of the entire Deesis tier on a single wooden panel. The iconography of the depicted artwork is in the traditional Novgorodian style. The painting had arrived at the STG heavily soiled with traces of soot and wax stains, along with some areas suspected to have undergone biodeterioration (Fig. 1). The latter could be attributed to its storage conditions in an unheated church, with unregulated fluctuations in humidity and temperature.

In January 2023, fifteen microbiological samples located in identified problem and control areas of the icon were collected from its surface and sides, as previously described [15]. Along with bacteria, the dominant representative destructor and sole fungal species was identified as *Iodophanus* sp. STG-150 (*Pezizaceae, Pezizales, Pezizomycetidae, Pezizomycetes, Pezizomycotina, Ascomycota*), described previously [15], which was detected throughout the painting's surface. The most common mould fungi that are known to damage paintings belong to the genera *Alternaria, Aspergillus, Cladosporium*, and *Penicillium* [16–18]. Other reported cases of biodegradation caused by fungi include those from the genera *Aureobasidium, Trichoderma, Pestalotiopsis*, and *Ustilago* [16], along with xerophilic fungi such as *Aspergillus creber* [19], *A. halophilicus, A. domesticus, A. magnivesiculatus*, and *A. vitricola*, which are able to grow in low-water conditions [20].

Fig. 1. Samplings from the icon "Deesis tier of 13 figures": four fragments (enlarged) indicated by green dots had craquelures, drips, and paint chips demonstrating conjoint fungal and bacterial growth.

Table 1
Antiseptics tested against *Iodophanus* sp. STG-150.

Antiseptics	Structural formula
Nucleoside derivatives	Ala 54; Ala106; SOV4
Sulphur-containing heterocyclic compounds	M1; M2; M3; M4
H-phosphinic amino acid analogues	Met-P_H; Ala-P_H; Val-P_H; Asp-α-P_H
Standard antiseptics (as controls)	BAC; NaPCP

n = 8,10,12,14,16,18

The present study was the first to identify a fungus from the *Pezizaceae* family in such an unusual habitat, along with its previously unheard-of predominance over the entire surface of the painting. In contrast, previously described *Iodophanus* isolates were commonly found on the manure of herbivores (cows, rabbits, etc.) and other decomposable natural cellulosic substrates [21,22]. Consequently, this study investigated the behaviour of *Iodophanus* sp. STG-150 on specific art materials and reported on the efficacy of novel antifungal agents to treat contaminated artworks.

2. Research aim

This study investigated the ability of the microscopic fungus *Iodophanus* sp. STG-150—isolated from the 16th century icon "Deesis Tier of 13 Figures"—to biodegrade mock layers composed of art materials such as varnishes, tempera pigments, adhesives, and binders, which are integral to the composition of the painting. Additionally, this study aimed to develop novel biocides that were effective against the fungal biodegradation, while simultaneously being non-toxic to art restaurateurs.

3. Materials and methods

3.1. Design and inoculation of mock layers

The mock layers were developed with modern analogues of art materials that were used in tempera paintings in the 16th century, according to literature sources [23]. The structure of the art layers was the same as previously described: linden board (support) was covered with canvas (pavoloka) and glued with ground layer (water solution of chalk and sturgeon glue, 70 g/l; afterwards different art materials was covered above [24]. The list of materials was classified into three groups: i) linen pavoloka, sturgeon glue (30 g/l), as well as sturgeon glue with antiseptic benzalkonium chloride (BAC, 1 %), and adhesives and binders (egg yolk emulsion consisting of egg yolk, water, and dry white wine [1:2:1]); ii) the colour palette comprising six dry tempera pigments of pure colours (ochre, cobalt green, strontium yellow, cadmium red, grey-green, zinc white) and four mixed colour pigments (zinc white and burnt sienna, zinc white and golden ochre, burnt sienna and shellac, as well as cobalt green and burnt sienna) in egg yolk emulsion; one pigment was an exception—watercolour black (madder, burnt azure, and soot) with gum arabic as a plasticizer; and iii) varnishes (such as acrylic varnish or linseed oil) and mordant as an adhesive for gilding. Each mock layer was divided into several equal fragments, approximately measuring 2 × 2 cm (Fig. S1).

Inoculation of the mock layers with *Iodophanus* sp. STG-150 was performed as previously described [24]. Before inoculation fragmented pieces were placed into sterile Petri dishes and saturated with 0.3 ml H2O per 1 cm^3 at 25 °C for 48 h, pieces with mock layers were placed on sterile hydrophobic spacers so that the lid of Petri dish did not touch the surface of the fragment. And then inoculated with fungi suspension of optic density (OD_{600}) = 1. Subsequently, the fungal growth on mock layers was measured every 6 days over a period of 36 days. The relative average growth area (AGA) was determined by the following formula:

$$AGA\,\% = [S_{tav}/S_c] \times 100$$

Wherein, S_{tav} indicates the average growth area (mm^2) obtained from the values on days 6, 12, 18, 24, and 30; S_c indicates surface area of the mock layer in mm^2. The data recorded were measured in triplicate and repeated at least twice.

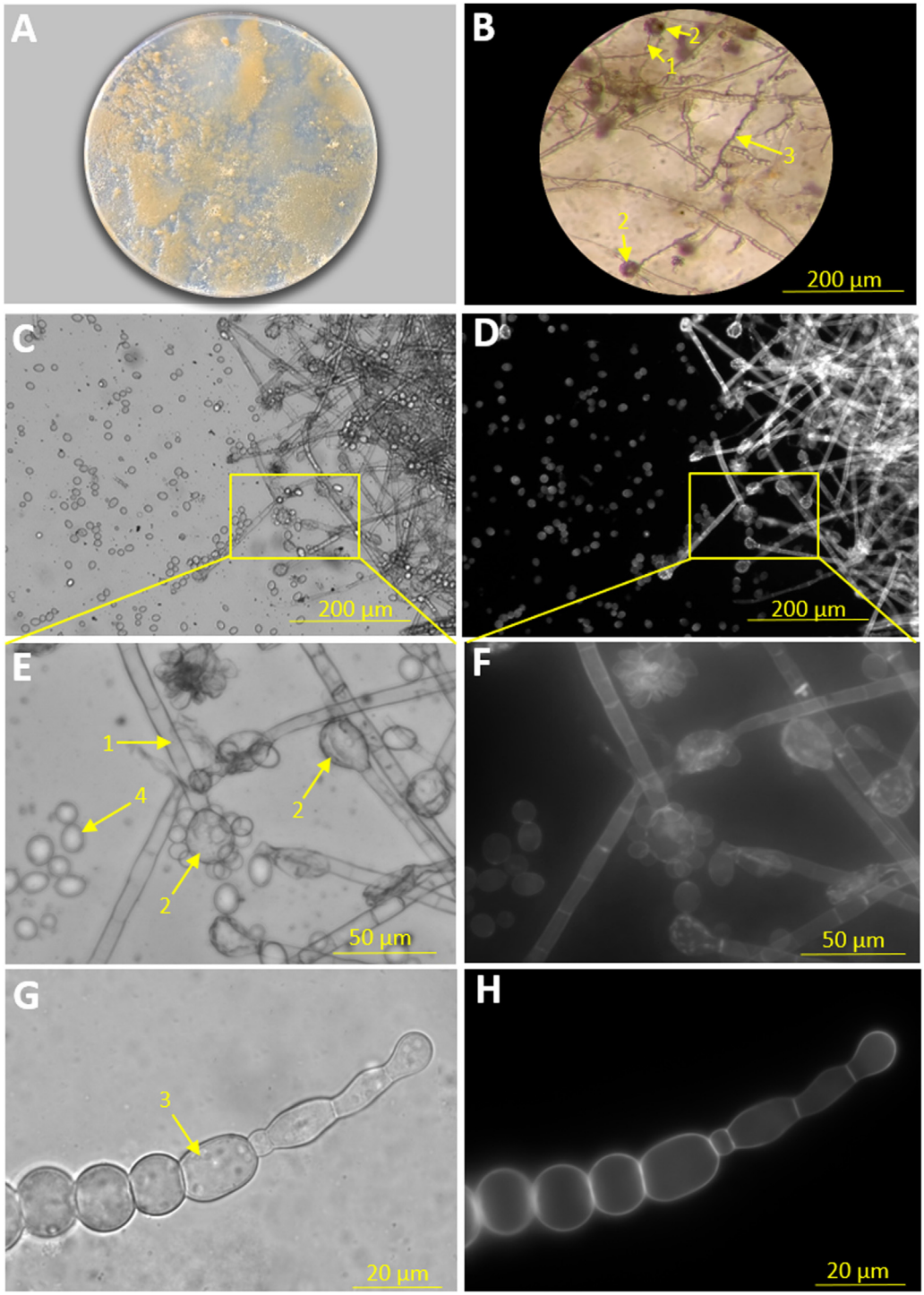

Fig. 2. Morphological forms of *Iodophanus* sp. (**A**) *Iodophanus* sp. STG-150 cultivated on PDA medium; (**B**) Lateral view via light microscopy clearly exhibited two morphological forms—aerial mycelium with conidiophores (1), vesicles (2), and vegetative mycelium in chains (3), 200 µm; (**C, D**) Transmission light and fluorescent microscopy of aerial mycelium, 200 µm; (**E, F**) Conidiophores (1), vesicles (2), and conidia (4), 50 µm; (**G, H**) Transmission light and fluorescent microscopy of vegetative mycelium in chains (3), 20 µm.

3.2. Morphological analysis *of* iodophanus *sp. STG-150*

Conidiospores and hyphal morphology of *Iodophanus* sp. STG-150 grown on potato dextrose agar (PDA, g/l: potato extract (200 r) – 4, glucose – 20, agar – 20, pH 5.6) and mock layers were detected using a LEICA M165 FC Fluo stereo microscope (LEICA, Germany) and a Celena X microscope (Logos biosystems, Korea). Additionally, Calcofluor White (CFW; Sigma-Aldrich, USA) was used as a fluorescent dye and the filters were adjusted as described: excitation filter 375/28, emission filter 460/50, lens plan apo fluor oil coverslip corrected 100 × NA 1.25, WD 0.19.

3.3. Scanning microscopy and spectral characteristics of mock layers

3.3.1. Scanning electron microscopy (SEM)

The surface microstructure of the mock layer samples inoculated with *Iodophanus* sp. STG-150 was examined using a Tescan AMBER FIB-SEM ion-beam scanning electron microscope (Tescan

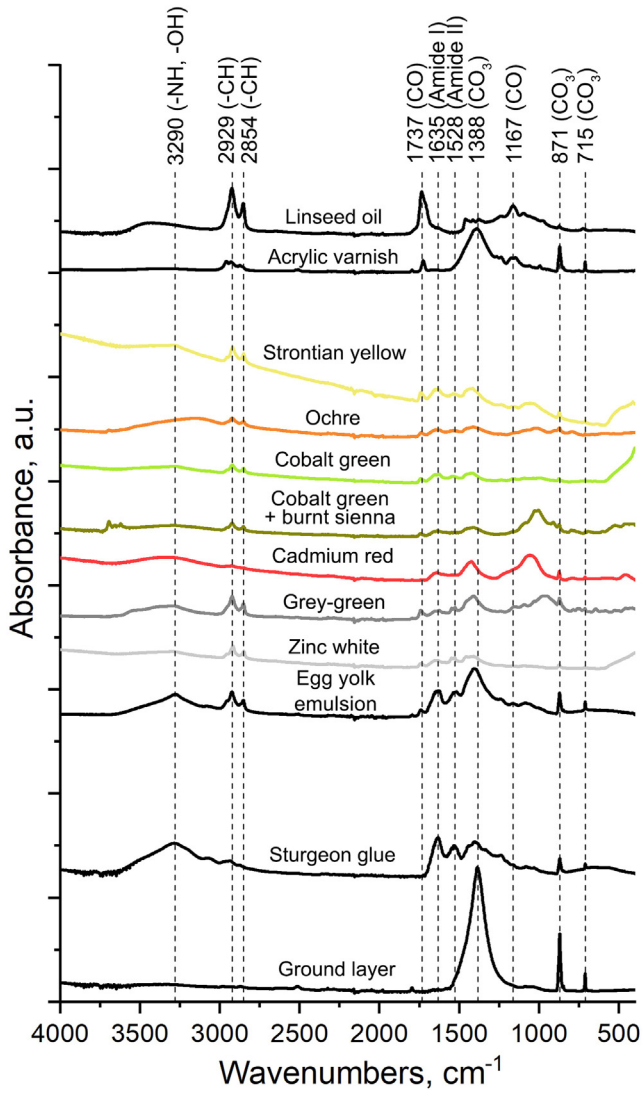

Fig. 3. FTIR spectra of the intact mock layers.

Group, Czech Republic). The sample containing paint flakes, along with the fungus, was extracted from the centre of the inoculation zone. An Everhart-Thornley secondary electron detector was used for SEM and the accelerating voltage was set to 1 keV. The focal length ranged from 5.5 to 6.0 mm. To intensify the charge flow, a carbon film was applied to the surface of the materials under analysis using a compact desk carbon coater (DCR, NanoStructured Coatings Co., Iran).

3.3.2. Fourier transform infrared (FTIR) spectroscopy

Infrared spectra of the intact and inoculated mock layers were acquired using a Nicolet iS50 spectrometer (Thermo Fisher Scientific, USA) in the wavenumber range from 400 to 4000 cm^{-1} in the attenuated total reflection mode. Two zones were defined for the analysis of inoculated mock layers: (i) the centre of inoculation, and (ii) the periphery zone - distance 1 cm from the center. Each final spectrum represented an average of 50 individual spectra obtained from a given sample area. Spectra were processed and analysed using the OMNIC software (Thermo Fisher Scientific, USA).

3.4. Antifungal activity

Antifungal activity was measured on PDA nutrient medium against three groups of substances—(i) nucleoside derivatives: N^4-dodecyl-5-methyl-2′-deoxycytidine (Ala 54) [25], N^4-dodecyl-5-methylcytidine (Ala 106) [26], and 3′-amino-N^4-dodecyl-5-methyl-2′,3′-dideoxycytidine (SOV4) [27]; (ii) sulphur-containing heterocyclic compounds: 3,5-dinitropyridin-2-yl thiocyanate – CAS 89465–95–2 (M1) [28], 4-nitro-2,1,3-benzothiadiazol-5-yl thiocyanate – CAS 91808–76–3 (M2) [29], 3-cyano-5-nitropyridin-2-yl thiomorpholine-4-carbodithioate – CAS 1446029–26–0 (M3) [30], and ethyl 1–hydroxy-6-thioxo-1,6-dihydropyridine-3-carboxylate – CAS 3061634–40–7 (M4) [31]; as well as (iii) *H*-phosphinic amino acid analogues: 1-Aminoethyl-*H*-phosphinic acid (Ala-pH) and L-amino-2-methylpropyl-*H*-phosphinic acid (Val-pH) were synthesized as per published protocols [32]; 1-amino-3-methylthiopropyl-*H*-phosphinic acid (Met-pH) was synthesized as described [33]; and L-amino-2-carboxyethyl-*H*-phosphinic acid (Asp-α-pH) was synthesized following previously published methodology [34]. Standard antiseptics used for comparison included Na Pentachlorophenate (NaPCP) and BAC, and PDA medium without any additives was used as the control (Table 1). All substances were tested at sublethal concentrations that facilitated the assessment of their respective antifungal effects. In particular, it was previously elucidated that 0.2 mM was a very effective concentration for Ala 54 and Ala 106 [26,27]. Furthermore, antifungal activity was evaluated based on the area of mycelial growth and apothecia formation.

Fungal growth inhibition (FGI) was determined by the following formula:

$$FGI\,\% = [(D_c - D_t)/D_c] \times 100$$

Wherein, D_c and D_t are areas with fungal growth on the control PDA media with no additives and experimental area on the PDA with antiseptics, respectively. The recorded data were measured in triplicate and repeated at least three times.

4. Results

4.1. Morphological characteristics *of* iodophanus *sp*

The microscopy results revealed a clear differentiation into vegetative (Fig. 2B, G, H) and aerial mycelium (Fig. 2B–D, E, F) in *Iodophanus* sp. STG-150, along with conidia formation on conidiophores, which was clearly visible via transmission light microscopy as well as with CFW in fluorescent microscopy. *Iodophanus* sp. STG-150 as a representative of the order *Pezizales* formed aerial mycelium under favourable conditions, when cultivated on PDA medium in the presence of constant light. The conidia were produced exogenously at the tips of the erect conidiophores (Fig. 2E–F).

4.2. Spectral characteristics of mock layers

The FTIR spectra of all the intact layers exhibited clear differences in their chemical composition (Fig. 3, Table S2). In particular, the ground layer was characterized by three major absorption bands (with maxima at approximately 715, 871, and 1388 cm^{-1}) related to the vibrations of the carbonate group of the main component ($CaCO_3$). The same signals (sometimes with a slight shift in the wavenumber) also appeared in the spectra of most other materials, which may be due to the features of the spectral recording technique used. The spectra of sturgeon glue contained the Amide I (~1635 cm^{-1}) and Amide II (~1528 cm^{-1}) bands, whereas for egg yolk they were supplemented by a signal from the carbonyl group (~1737 cm^{-1}). All of the above absorption bands are usually observed in the spectra of paint layers. In the case of acrylic varnish, the signal from the carbonyl group was more pronounced. Furthermore, the carbonyl group exhibited the dominant signal in the spectrum of linseed oil, along with the absorption bands of OH

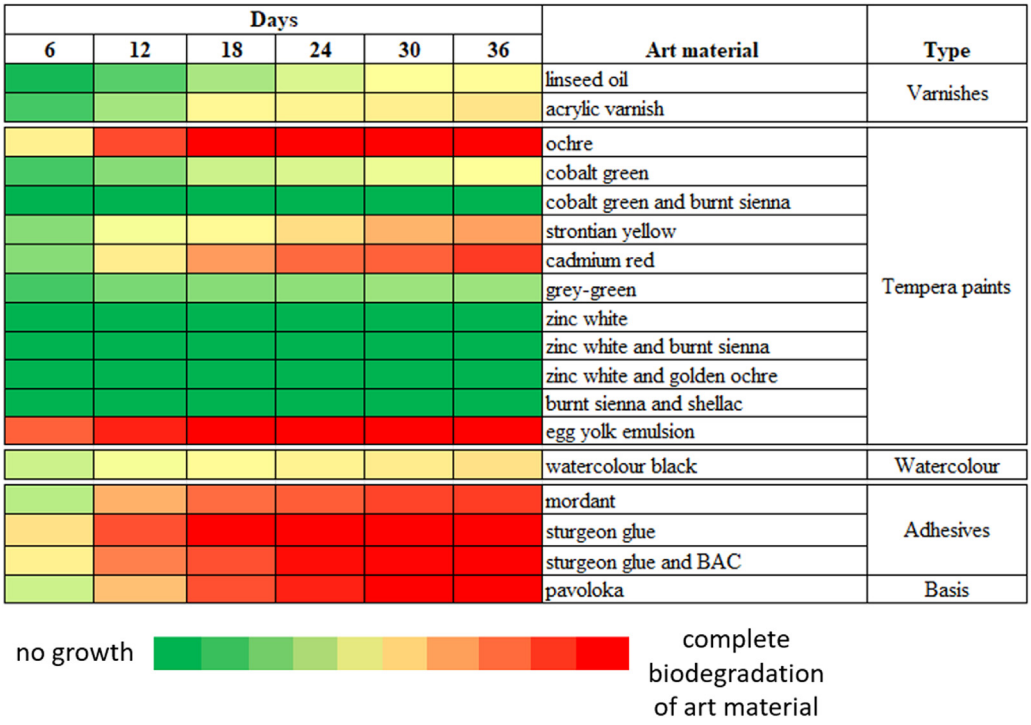

Fig. 4. Dynamics of biodegradation of the mock layers composed of different art materials by *Iodophanus* sp. STG-150 after 6, 12, 18, 24, 30, and 36 days post-inoculation.

groups and a signal with a peak at 1167 cm^{-1}, which was related to the stretching vibrations of the C–O group in triglycerides ester and higher aliphatic esters [35].

4.3. Inoculation of mock layers

Direct examination of the selected mock layers inoculated with *Iodophanus* sp. STG-150 confirmed the ability of fungus to colonize the material with varying degrees of propensity. Confident colonization with the mycelium and apothecium formation was observed after 48 h on the following six members: with egg yolk emulsion, mordant, sturgeon glue and sturgeon glue with antiseptic BAC, pavoloka, as well as ochre pigment. This group demonstrated high growth intensity, wherein the area of the mycelium coverage was approximately 14–20 mm at the end of the experiment. The other group with moderate to low growth intensity included seven constituents: linseed oil and acrylic varnishes, four tempera pigments (cobalt green, strontian yellow, cadmium red, and grey-green), as well as watercolour black, with the area of the mycelium coverage measuring 2–10 mm. Additionally, the final group in which fungal development was practically undetectable comprised five components: zinc white as well as all layers with combinations of zinc white and burned sienna (Fig. 4).

For a more visual representation, Fig. 5 depicts the averaged data on fungal growth on mock layers, based on the average area of biodegradation over the entire observation period of 36 days.

The mock layer with egg yolk emulsion after inoculation with *Iodophanus* sp. STG-150 revealed shiny fruiting bodies of beige-pink colour in the inoculation zone. During the 12-day period, *Iodophanus* sp. STG-150 had utilized nearly 90 % of the egg emulsion and expanded onto the protruding fibres of the canvas, each of which was covered with fluffy light mycelium (most likely aerial). Furthermore, SEM revealed the formation of conidiophores with conidia on vesicles, as well as strands of vegetative mycelium seemingly in the depths behind the aerial mycelium (Fig. 6B, C).

The mock layer with ochre-pigment revealed shiny fruiting bodies of beige-pink colour in the central inoculation zone (i), with the same morphology as observed on egg yolk. Additionally, concentric circles of a lighter colour were present around the fruiting bodies, which were presumably threads of aerial mycelium. An image of the vegetative mycelium, along with pinched conidia of aerial mycelium on top of it, was also obtained via SEM (Fig. 7B, C).

The spectrum of the intact ochre layer is very similar to that of the egg yolk emulsion (Fig. 3, Table S2) with respect to the sets of absorption bands observed, which may be attributed to the presence of the same binder in its composition. Thus, both of these materials exhibited absorption bands with maxima at approximately 1635 and 1528 cm^{-1}, related to Amide I and Amide II. Moreover, quite intense bands were formed at 871 and 1415 cm^{-1}. These were possibly associated with the vibrations of the carbonate groups present in $CaCO_3$, which was a component of the ground layer. Notably, the spectra of the intact ochre and egg yolk also contained a spectral marker at approximately 1737 cm^{-1}, which related to the absorption of carbonyl groups [36]. Therefore, this absorption band was absent in the spectrum of ochre in the centre of the inoculation zone (i) and had low intensity in the case of ochre in the periphery zone (ii). This indicated a significant decrease in the concentration of C=O groups in the composition of the materials and illustrated the development of the fungal infection in the centre (i) of the inoculation as well as at the 1 cm peripheral zone (ii) (Fig. 7D). There was also a decrease in the intensity of the absorption bands of OH groups and an intensification in the signals obtained from the ground layer for ochre from both the (i) and (ii) samples.

On the mock layer with cobalt green-pigment, it was possible to distinguish the sparse rounded, shiny fruiting bodies of *Iodophanus* sp. STG-150 with a beige-pink colour, in the inoculation zone (i) (Fig. 7A). Furthermore, SEM microphotography revealed a film-like ectal excipullum of the fungus in this zone (i), which appeared in the form of garlands with a wrinkled pineal shape that was clearly distinguishable at 20 μm (Fig. 8B, C).

The spectra obtained for cobalt green (Fig. 8D) illustrated the development of fungal infection in the centre of inoculation (i) as well as at the 1 cm-wide periphery zone (ii). These spectra

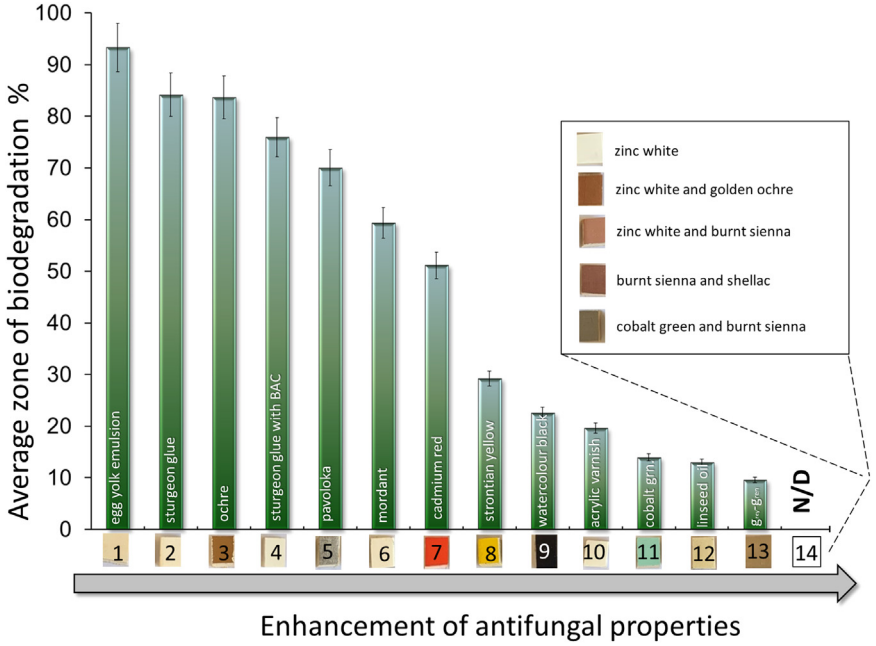

Fig. 5. Average values of the biodegradation zones (% of the total area) following the cultivation of *Iodophanus* sp. STG-150 on the mock layers with colourings. 1–egg yolk emulsion; 2–sturgeon glue; 3–ochre; 4–sturgeon glue with BAC; 5–pavoloka; 6–mordant; 7–cadmium red; 8–strontian yellow; 9–watercolour black; 10–acrylic varnish; 11–cobalt green; 12–linseed oil; 13–grey-green; and 14–zinc white, or zinc white and golden ochre, or zinc white and burnt sienna, or burnt sienna and shellac, or cobalt light green and burnt sienna. N/D, not detected. Data has been presented as the mean ± SD, $n = 3$.

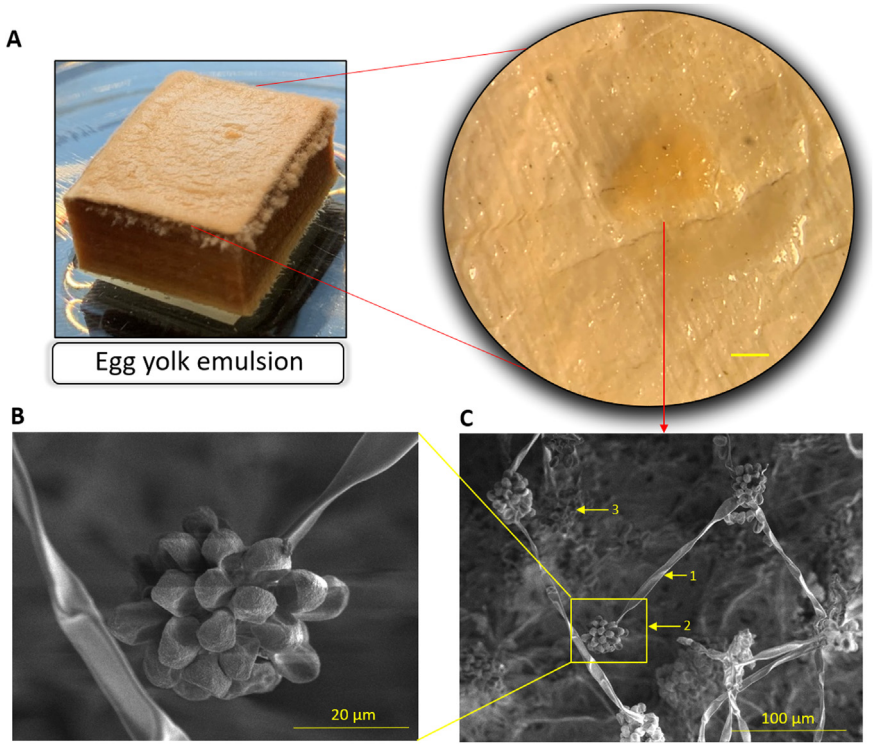

Fig. 6. Morphological characteristics of *Iodophanus* sp. STG-150 inoculated on the mock layer with egg yolk emulsion and BAC. The photos were captured on the 12th day post inoculation. (**A**) Mock layer with egg yolk emulsion and its lateral view via light microscopy, 1.8 mm; (**B**) SEM image of conidiophores with conidia; (**C**) SEM image of conidiophores (1), vesicles with conidia (2), and strands of vegetative mycelium (3).

primarily differed from the spectrum of the intact layer in the intensification of spectral markers from the ground layer, which was indicated by the disappearance of the signal from the carbonyl group as well as an increase in the intensity of the complex absorption band in the region of 900–1200 cm^{-1}. The latter was characteristic of polysaccharides present in the cellular structure of fungi. Consequently, these observations allow us to trace the dynamics of biodegradation on the periphery from the inoculation zone.

Other mock layers with sturgeon glue (Fig. S3), strontian yellow (Fig. S4), watercolour black (Fig. S5), mordant (Fig. S6), acrylic varnish (Fig. S7), zinc white (Fig. S8) revealed the presence of only

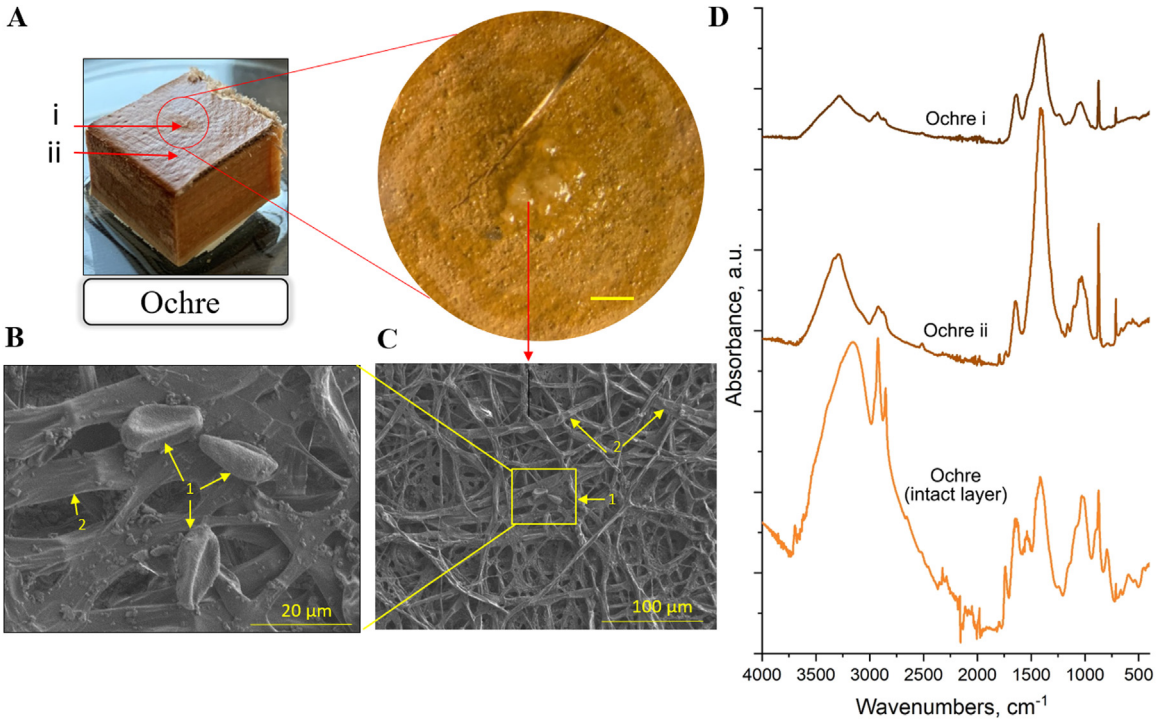

Fig. 7. Morphological and spectral characteristics of *Iodophanus* sp. STG-150 inoculated on a mock layer with ochre pigment. The photos were captured on the 12th day post inoculation. (**A**) Mock layer with ochre pigment and its lateral view via light microscopy, 1.8 mm; (**B, C**) SEM images of pinched conidia (1) and strands of vegetative mycelium (2); (**D**) FTIR spectra of the ochre pigment: (i) the centre of the inoculation zone, (ii) periphery zone—1 cm, intact ochre layer prior to inoculation.

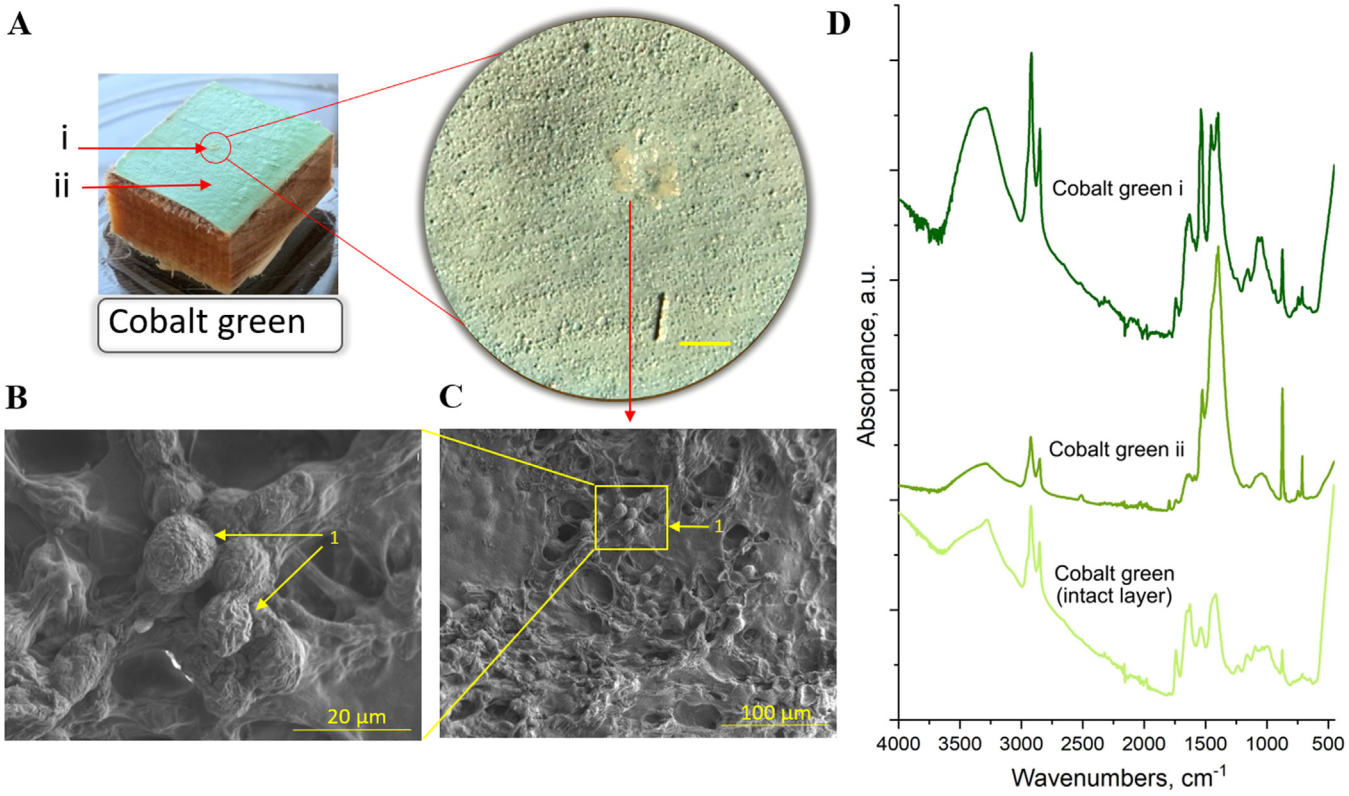

Fig. 8. Morphological and spectral characteristics of *Iodophanus* sp. STG-150 inoculated on a mock layer with cobalt green pigment. The photos were captured on the 12th day post inoculation. (**A**) Mock layer with cobalt green and its lateral view via light microscopy, 1.8 mm; (**B, C**) SEM images of film with vegetative mycelium (1); (**D**) FTIR spectra of the cobalt green pigment: (i) the centre of the inoculation zone, (ii) periphery zone—1 cm, intact layer of cobalt green prior to inoculation.

the vegetative mycelium directly in the centre of the inoculation zone, with varying degrees of density 30 days post-inoculation. It was not possible to visualize living structures of the fungus on the mock layer with zinc white-pigment (Fig. S8), unlike the other art materials described above. Furthermore, SEM detected a scanty number of lifeless structures, which were presumably a dehydrated film of mycelium (Fig. S8). Additionally, oval structures—most likely belonging to inorganic particles of the pigment zinc white—were observed beside the mycelium strand.

The FTIR spectra for acrylic varnish (i) and (ii) in comparison with the corresponding intact layer (S 7 Fig) revealed biodegradation in the periphery zone initiated from the inoculation zone. This phenomenon was manifested by the gradual disappearance of the absorption band around 1737 cm^{-1} (carbonyl group), as along with the appearance of the Amide I and Amide II bands as well as an absorption band in the region of 900–1200 cm^{-1} from polysaccharides, which may be attributed as the spectral markers of the selected fungus.

4.4. Antifungal activity

The study investigated the antifungal activity of several novel biocides from a series of nucleoside derivatives, sulphur-containing heterocyclic compounds, and *H*-phosphinic amino acid analogues in *Iodophanus* sp. STG-150 grown on PDA nutrient medium with two standard antiseptics, along with a separate control without any antiseptics. Consequently, it was observed that Ala 54 and Ala106—despite their reported effectiveness against a number of fungi, such as *A. versicolor* STG-25, *A. creber* STG-57, *Ulocladium* STG-36 sp. AAZ-2020a, and *C. halotolerance* STG-52B, etc. [25]—could not limit the growth of *Iodophanus* sp. STG-150 and were ineffective as antifungal agents. In contrast, SOV 4 was more effective; however, the fungus was able to overcome its fungistatic effects after 9 days (Fig. 10). Interestingly, the *H*-phosphinic amino acid analogue of valine (Val-pH) altered the morphology of the fungus (Fig. 9), but was not very active as a fungicide. Conversely, compounds such as M1–M4 and the *H*-phosphinic analogue of aspartate (Asp-α-pH) completely restricted the growth of the fungus at a concentration of 0.2 mM, as compared to NaPCP and BAC (Fig. 9).

Furthermore, an illustration of FGI (%) on PDA medium with 0.2 mM of antiseptics in comparison with the control (no additives) has been presented in the form of a thermogram, wherein the green grids correspond to the presence of fungal growth, and the red ones indicate its complete inhibition (Fig. 10).

5. Discussion

5.1. Dynamics of mock layer biodegradation *along* with its spectral characteristics

The predominant cases among the mock layers subjected to biodegradation by *Iodophanus* sp. STG-150 were egg yolk emulsion and ochre pigment, both of which exhibited dense salmon pink-coloured mycelium (Fig. 6A, Fig. 7A). Additionally, characteristic morphological forms belonging to the aerial mycelium on egg yolk (Fig. 6B, C), as well as individual pinched conidia on ochre pigment (Fig. 7B, C) were observed. Ochres belong to the earth pigment group that comprises iron oxide- and hydroxide-rich earths varying in colour from brown and reds through yellows [37]. Apparently, tempera ochre in egg yolk has the maximum bioavailability for the growth and development of *Iodophanus* among studied pigments, as detected spectrally (Fig. 7D).

The cobalt green mock layer demonstrated the presence of only the ectal excipulum of the fungus directly in the inoculation zone. Furthermore, its spherical globules were wrinkled and pineal-shaped, which possibly indicated growth inhibition in the fungus (Fig. 8B, C). Despite the difficulty in visualising the biodegradation at the periphery of the inoculation zone, even a minor presence of biomaterial can be detected spectrally through FTIR (Fig. 8D). Moreover, it must be taken into consideration that when an artwork is exposed to unfavourable conditions with uncontrolled temperature and humidity, even a minor presence of mycelium and spores can contribute to a full-fledged fungal infection.

The mock layer with watercolour black—comprising a mix of water-soluble coloured pigments such as madder, burnt azure, and soot in gum arabic as plasticizer—demonstrated a mild but persistent development of the fungus apothecium after inoculation (Fig. S5). The intensity of biodegradation strongly depends on the composition of art materials. Consequently, it is possible that *Iodophanus* sp. STG-150 contains the appropriate enzymes that are capable of hydrolysing the polysaccharides present in gum arabic.

Furthermore, the mock layer with oil-based mordant [38]—used in iconography for the gilding background elements, halos, rays of light, draperies and other details—also exhibited mycelial growth on its surface (Fig. S6). Presumably, the fungus was able to develop on the material due to the organic nature of this adhesive. Moreover, protective varnishes such as acrylic (Fig. S7) also revealed the development of mycelium at the end of the experiment, which could potentially be attributed to the appearance of micro cracks in the surface of the material under experimental conditions that simulated an emergency situation representing high humidity conditions. Therefore, the inoculated fungus was able to penetrate the cracks after approximately 10 days and began to grow, which was further confirmed via spectral analysis (Fig. S7).

In contrast, the mock layers with zinc white pigment revealed a dried film of fungal mycelium (Fig. S8). The low growth rate of *Iodophanus* sp. STG-150 on this pigment can most likely be explained by the general toxicity of heavy metal ions—such as Zn^{2+}—in microorganisms [39,40]. In this regard, morphological alterations such as hyphae damage following treatment with Zn compounds have been demonstrated against certain toxigenic strains of *Fusarium graminearum, Penicillium citrinum*, and *Aspergillus flavus* [41]. Other combinations of zinc white with earth pigments such as golden ochre and burned sienna exhibited no fungal development on their surfaces after inoculation, possibly due to the greater toxic impact of zinc itself than the other components.

Consequently, it can be concluded that the *Iodophanus* sp. STG-150 prefers some pigments over others for its successful colonization in artworks. This also correlates with the data we obtained earlier [24]. Although the pigment pallet in current work is slightly differ from those studied previously, the repeated paint layers (ochre pigment, egg yolk emulsion, and sturgeon glue) exhibited a similar tendency. Natural egg tempera and ochre pigment were some of the best substrates for microbial growth, as they were quickly colonized (within 2–5 days) with most of the inoculated fungi belonging to the classes *Eurotiomycetes, Sordariomycetes*, and *Dotideomycetes.* Next in terms of degradation rate was sturgeon glue, which was broken down at varying rates by different representatives of the same fungal classes [24]. However, all of them bore a resemblance to *Iodophanus* sp. in the complete degradation of the sturgeon glue within approximately 12–18 days.

In the case of earlier investigation of a 17th century easel painting, it was demonstrated that the distribution of the fungi was different across various coloured areas of the painting [42]. In particular, *Aspergillus* spp. and *Penicillium* spp. were detected on dark-brown and red-coloured areas, whereas *Cladosporium* spp. was observed in samples extracted from lighter areas with yellow and ruddy pink pigments [42]. Consequently, the biodegradative poten-

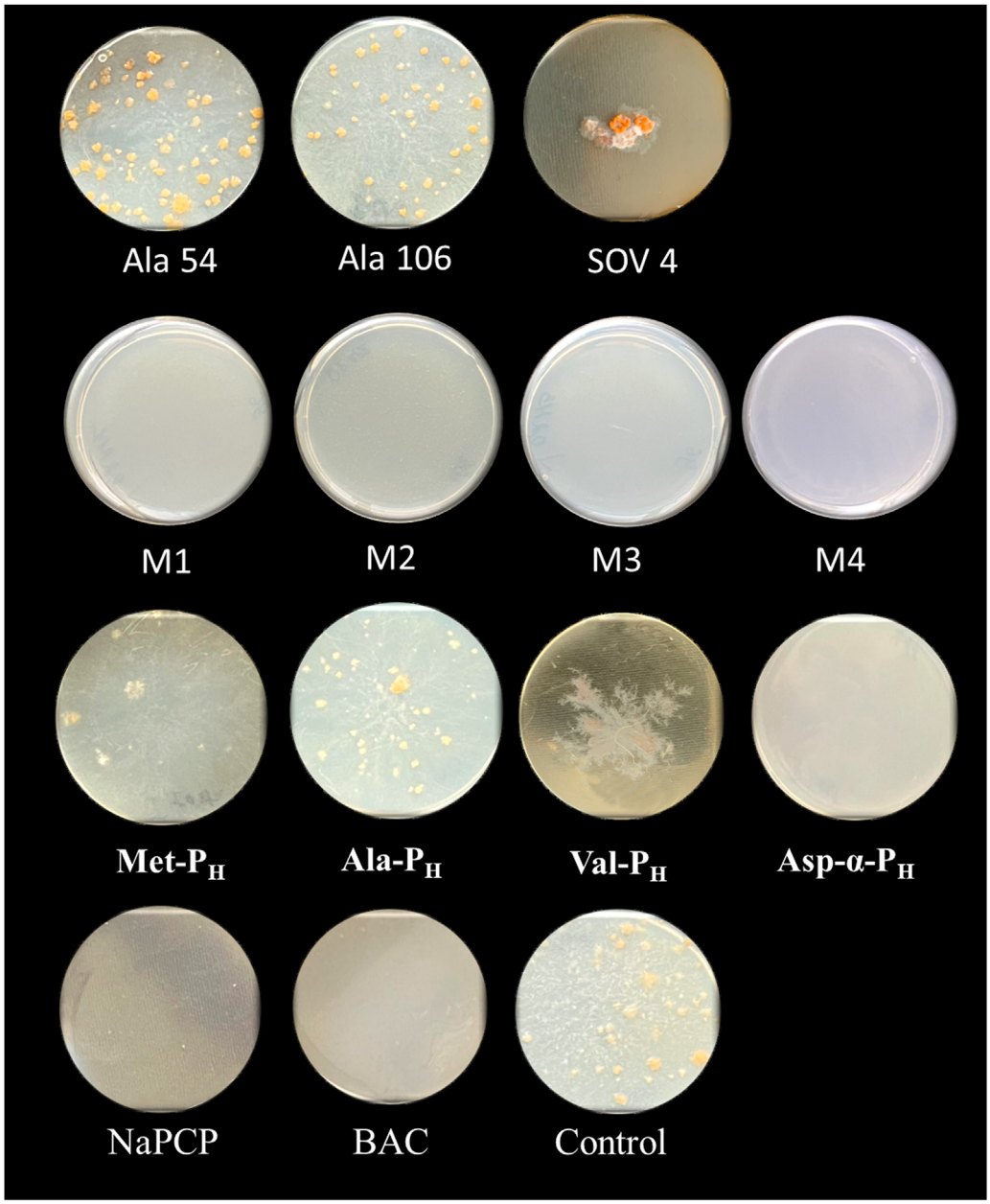

Fig. 9. The phenotype of *Iodophanus* sp. STG-150 on PDA medium, supplemented with 0.2 mM NaPCP, or BAC, and with 0.2 mM of nucleoside derivatives (Ala 54, Ala 106, SOV 4), sulphur-containing heterocyclic compounds (M1–M4), and *H*-phosphinic amino acid analogues (Met-P_H, Ala-P_H, Val-P_H and Asp-α-P_H). Petri dishes were captured 40 days post-inoculation.

tial of different fungi for certain pigments clearly depend on their enzymatic profile [12].

5.2. Antifungal activity of novel derivatives

Despite intensive research, the biological targets and mechanism of action of 5-modified 2′-deoxynucleoside derivatives and N^4-modified cytidine derivatives have not yet been identified. However, it is suggested that the possible mechanism of action of this type of nucleosides may be their direct or indirect effect on the cell wall of microorganisms. This is based on previous data [43] from *Mycobacterium tuberculosis* cells, wherein the addition of 5-substituted pyrimidine nucleosides led to distinct alterations in the morphology of bacterial cells as well as their destruction. Furthermore, a recent study [44] demonstrated that lipophilic derivatives of 2′-deoxyuridine and cytidine are capable of destroying artificial membranes created on the basis of various lipids—including mycolic acids—which are part of the mycobacterial cell wall. Simultaneously, the potent antifungal effects of Ala 54 and Ala 106 at a concentration of 0.2 mM has been demonstrated against certain fungal strains such as *Penicillium chrysogenum* STG-117, *Cladosporium parahalotolerans* STG-93B, *C. halotolerants* STG-52B, *Microascus paisii* STG-103, *Simplicillium lamellicola* STG-96, and *Ulocladium* sp. STG-36, along with partial effects against *Aspergillus* and *Mucor* species [26]. Presumably, these compounds can exhibit fungicidal activity against *Iodophanus* sp. STG-150 as well, but only SOV4 could inhibit its growth to approximately 80 % only till the 9th day at the same concentration. Earlier, we had also demonstrated the complete inhibition by 0.7 mM SOV4 of the same fungi as mentioned above, including *Aspergillus* and *Mucor*, but excluding *Penicillium chrysogenum* and *Simplicillium lamellicola* [27].

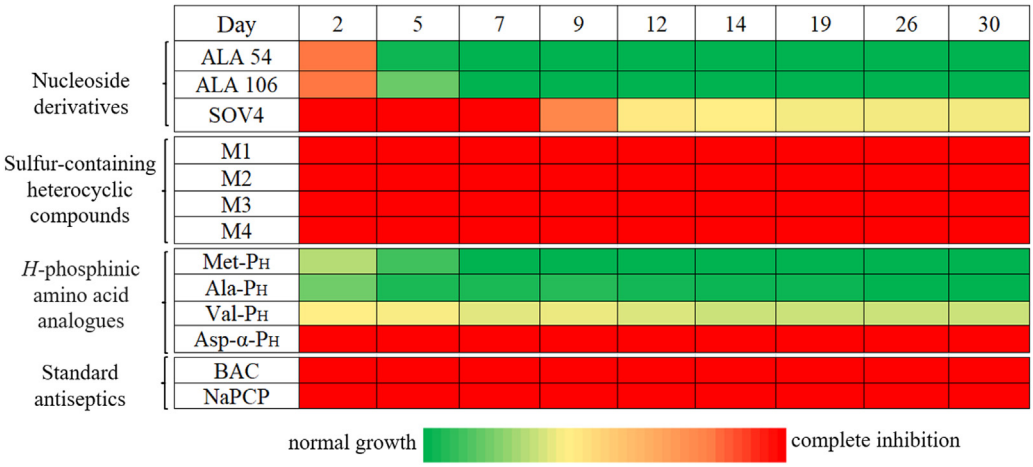

Fig. 10. Dynamics of *Iodophanus* sp. STG-150 growth inhibition on PDA medium with 0.2 mM analogues of nucleosides, sulphur-containing heterocyclic compounds, and *H*-phosphinic amino acid analogues or 0.2 mM of standard antiseptics NaPCP and BAC as the control, measured 2, 5, 7, 9, 12, 14, 19, 26, and 30 days post-inoculation.

Till date, the antifungal mechanism of the compound 3,5-dinitropyridin-2-yl thiocyanate (M1) has not been clearly elucidated. Its action may potentially be associated with a disruption of the structure of the fungal cell wall, thereby resulting in pathological changes, and possibly even its rupture.

The antimicrobial properties of pyridine derivative M2 have been previously published [45], whereby it was determined that it inhibits cell division by blocking FtsZ GTPase activity. Furthermore, its microbial antibiofilm activity was demonstrating using microtiter plates, confocal microscopy, and an in vitro biofilm wound model. Previous results also indicated that the compound M2, which is an FtsZ inhibitor, exhibits toxic activity against a wide range of *S. aureus* strains. However, the precise mechanism of antifungal action is not fully understood. In our preliminary experiments, we demonstrated that compound M2 inhibits gamma glutamylcysteine synthetase, which catalyses the first step in the gamma-glutamyl cycle involved in fungal glutathione biosynthesis.

The broad spectrum of antifungal activity exhibited by M3—a 5-nitropyridin-2-yl-thioalkenyl-4-dithiocarbamate derivative—has been published as a patent [30], without any information about the exact cellular targets of these compounds. However, it can be presumed that M3 potentially targets fungal carbonic anhydrase. Moreover, several existing publications link this target to the antimicrobial and antifungal activity of dithiocarbamates [46,47].

Similarly, the antimicrobial properties of the compound M4 has been described in detail in a recent study [31], wherein its mode of action is comparable to that of compound M2, which inhibits FtsZ GTPase activity. It was previously elucidated that similar compounds possess specific properties that allow them to form complexes with Cu^{2+} captured from water or media. These complexes are forcibly transferred into the cells, where they destroy their components through the release of free cuprum. Consequently, this process exerts an overall toxic effect on microbial and fungal cells [48].

Certain α-amino-*H*-phosphinic acids exhibit antibacterial [49–51] and fungicidal activity against various pathogens of cultivated plants [52–55]. For instance, in the phytopathogenic fungus *Pyricularia oryzae*—which causes the foremost pathogenic rice-blast disease—Ala-pH is converted into an *H*-phosphinic analogue of pyruvate, which acts as an effective inhibitor of pyruvate dehydrogenase. This ultimately leads to the inhibition of Ac-CoA biosynthesis and Ac-CoA-dependent biosynthesis pathways, including melanogenesis [56].

However, Ala-pH was inactive against *Iodophanus* sp. STG-150 (Fig. 9), which is rarely associated with poor uptake of this analogue. Practically nothing is known about the Ac-CoA biosynthesis in *Iodophanus* sp. STG-150. Ac-CoA in this fungus may be derived from acetic acid, rather than from pyruvate, which is typical for many tumour cells [57,58].

In contrast, Met-pH demonstrated excellent fungicidal activity against *P. oryzae* in field trials [56]. However, Met-pH only exhibited moderate activity against *Iodophanus* sp. STG-150 (Fig. 9). The effect lasted for only 5 days, following which the fugal growth resembled the control (Fig. 10). Most likely, the peculiarities of the methionine metabolising enzymes in this fungus are the underlying cause for this.

Val-pH (Table 1) was much more active than Ala-pH and Met-pH in inhibiting the growth of *Iodophanus* sp. STG-150 mycelia by 45 % on day 30 of the experiment (Fig. 10). Addition of Val-pH to PDA medium altered the morphology of the fungus and resulted in significant inhibition of mycelial growth in agar (Fig. 9). The structural similarity of valine and Val-pH suggests that the analogue may target the enzymes of branch-chain amino acids metabolism, although very little is known about the metabolism of these amino acids in *Iodophanus* sp. STG-150.

Moreover, Asp-α-pH (Table 1) was the most active amongst all the compounds and completely inhibited the growth of *Iodophanus* sp. STG-150 throughout the entire 30 days of the experiment (Fig. 10). Presumably, the activity of Asp-α-pH against *Iodophanus* sp. STG-150 is not associated with the inhibition of Ac-CoA-dependent biosynthetic pathways, as Ala-pH is inactive. The relationship between the inhibition of the enzymes of dicarboxylic amino acid metabolism and the growth of *Iodophanus* sp. STG-150 remains to be elucidated. Notably, Asp-α-pH inhibited (IC_{50} 0.5 μg/mL) the growth of mycelium and germination of conidia of *Magnaporthe grisea* on agar medium, along with efficiently bleaching the mycelium [56].

6. Conclusions

This study demonstrated that the presence of the fungus *Iodophanus* sp. STG-150 on the surface of artworks is ubiquitous, but not uniform, as it prefers mainly ochre pigments. Red, yellow, cobalt-based green, and grey-green pigments are preferred to a lesser extent, whereas the fungus practically does not develop on zinc white. However, if cracks or crumbling are observed in the violation of the protective varnish coating of the icon, then *Iodo-*

phanus sp. STG-150 can penetrate the paint layer and develop deeper, especially preferring yolk emulsion, sturgeon glue and the basis pavoloka and wood itself, as cellulolytic substrates. Consequently, the biodegradative potential of *Iodophanus* sp. STG-150 indicates a high risk for the studied artwork, with respect to the intensity of its biodegradative activity, which primarily caused deterioration of the basis and the ground layers. Unfortunately, the antiseptic benzalkonium chloride traditionally used by restorers does not guarantee protection from this type of fungus. The use of novel biocides sulphur-containing heterocyclic compounds and *H*-phosphinic analogue of aspartate against biodegradation of *Iodophanus* sp. STG-150 was effectively demonstrated in this study, as they completely inhibited the growth of the fungus. Currently, limitations are associated with the practical possibility of using sulphur-containing heterocyclic compounds and *H*-phosphinic analogue only due to the scaling of their synthesis, since they are synthesized in laboratory conditions now in test mode.

Funding

This work was supported by the Russian Science Foundation (grant No. 25-28-00231).

Acknowledgements

The authors would like to thank the entire team of the tempera painting restoration workshop at the State Tretyakov Gallery for their cultural contribution. The authors would also like to express their gratitude to Mr. Evgeniu Avdanin for his design of Graphical Abstract.

Supplementary materials

Supplementary material associated with this article can be found, in the online version, at doi:10.1016/j.culher.2025.11.001.

References

[1] X. He, M. Xu, H. Zhang, B. Zhang, B. Su, An exploratory study of the deterioration mechanism of ancient wall-paintings based on thermal and moisture expansion property analysis, J. Archaeol. Sci. 42 (2014) 194–200, doi:10.1016/J.JAS.2013.10.035.
[2] Q. Li, B. Zhang, Z. He, X. Yang, Distribution and diversity of bacteria and fungi colonization in stone monuments analyzed by high-throughput sequencing, PLoS One 11 (2016) e0163287, doi:10.1371/journal.pone.0163287.
[3] M.M.E. Khalil, A.A.I. Mekawey, F.A. Alatawi, Microbial deterioration of the archaeological Nujoumi Dome (Egypt-Aswan): identification and suggested control treatments by natural products, J. Pure Appl. Microbiol. 16 (2022) 990–1003, doi:10.22207/JPAM.16.2.22.
[4] A. Pyzik, K. Ciuchcinski, M. Dziurzynski, L. Dziewit, The bad and the good-microorganisms in cultural heritage environments-an update on biodeterioration and biotreatment approaches, Materials (Basel) 14 (2021) 1–15, doi:10.3390/MA14010177.
[5] A. Pavić, T. Ilić-Tomić, A. Pačevski, T. Nedeljković, B. Vasiljević, I. Morić, Diversity and biodeteriorative potential of bacterial isolates from deteriorated modern combined-technique canvas painting, Int. Biodeterior. Biodegrad. 97 (2014) 40–50, doi:10.1016/j.ibiod.2014.11.012.
[6] C. Salvador, R. Bordalo, M. Silva, T. Rosado, A. Candeias, A.T. Caldeira, On the conservation of Easel paintings: evaluation of microbial contamination and artists materials, Appl. Phys. A Mater. Sci. Process. 123 (2017), doi:10.1007/S00339-016-0704-5.
[7] S. Capodicasa, S. Fedi, A.M. Porcelli, D. Zannoni, The microbial community dwelling on a biodeteriorated 16th century painting, Int. Biodeterior. Biodegrad. 64 (2010) 727–733, doi:10.1016/J.IBIOD.2010.08.006.
[8] S. Shrivastava, Biodeterioration of art objects on paper and their conservation, Res. J. Recent Sci. 4 (2015) 42–46.
[9] M. Chadeganipour, R. Ojaghi, H. Rafiei, M. Afshar, S.T. Hashemi, Biodeterioration of library materials: study of fungi threatening printed materials of libraries in Isfahan University of medical sciences in 2011, Jundishapur J. Microbiol. 6 (2013) 127–131, doi:10.5812/JJM.4751.
[10] S. Borrego, I. Vivar, Biological diversity detected in two deteriorated Cuban cinematographic films that contribute to their biodegrading, J. Microbiol. Exp. 12 (2024) 88–96, doi:10.15406/JMEN.2024.12.00421.
[11] A.R. Szczepanowska, H.M. Cavaliere, Artworks, drawings, prints, and documents - Fungi eat them all!, in: F.E. Koestler, R.J. Koestler, V.H. Charola, A.E. Nieto-Fernandez (Eds.), Art, Biology, and Conservation, The Metropolitan Museum of Art, New York, 2003, pp. 128–151.
[12] D. Văcar, C.L. Mircea, C. Pârvu, M. Podar, Diversity and metabolic activity of fungi causing biodeterioration of canvas paintings, J Fungi 8 (2022) 589, doi:10.3390/jof8060589.
[13] F, Y. Zhang, M. Su, F. Wu, J.-D. Gu, J. Li, D. He, Q. Guo, H. Cui, Q. Zhang, Huyuan, Diversity and composition of culturable microorganisms and their biodeterioration potentials in the sandstone of Beishiku Temple, China, Microorganisms 11 (2023) 429, doi:10.3390/microorganisms11020429.
[14] C. P, M. Wiszniewska, J. Walusiak-Skorupa, I. Pannenko, M. Draniak, Occupational exposure and sensitization to fungi among museum workers, Occup. Med. (Chic. Ill). 59 (2009) 237–242, doi:10.1093/occmed/kqp043.
[15] D.A. Avdanina, A.A. Ermolyuk, K.Y. Bashkirova, O.B. Vorobyova, N.P. Simonenko, M.V. Shitov, A.A. Zhgun, Determining the source of biodeterioration of the 16th century icon Deesis tier of 13 figures from the State Tretyakov Gallery, Microbiol. (Russian Fed. 93 (2024) S87–S92, doi:10.1134/S0026261724609345.
[16] G.M. Gadd, M. Fomina, F. Pinzari, Fungal biodeterioration and preservation of cultural heritage, artwork, and historical artifacts: extremophily and adaptation, Microbiol. Mol. Biol. Rev. 88 (2024), doi:10.1128/MMBR.00200-22.
[17] D.A. Avdanina, A.A. Zhgun, Rainbow code of biodeterioration to cultural heritage objects, Herit. Sci. 2024 121 (12) (2024) 1–24, doi:10.1186/S40494-024-01298-Y.
[18] K. Kavkler, M. Humar, D. Kržišnik, M. Turk, Č. Tavzes, C. Gostinčar, S. Džeroski, S. Popov, A. Penko, N. Gunde - Cimerman, P. Zalar, A multidisciplinary study of biodeteriorated Celje Ceiling, a tempera painting on canvas, Int. Biodeterior. Biodegradation. 170 (2022) 105389, doi:10.1016/J.IBIOD.2022.105389.
[19] A. Micheluz, S. Manente, V. Tigini, V. Prigione, F. Pinzari, G. Ravagnan, G.C. Varese, The extreme environment of a library: xerophilic Fungi inhabiting indoor niches, Int. Biodeterior. Biodegrad. 99 (2015) 1–7, doi:10.1016/J.IBIOD.2014.12.012.
[20] C.J. Bastholm, A.M. Madsen, B. Andersen, J.C. Frisvad, J. Richter, The mysterious mould outbreak - A comprehensive fungal colonisation in a climate-controlled museum repository challenges the environmental guidelines for heritage collections, J. Cult. Herit. 55 (2022) 78–87, doi:10.1016/J.CULHER.2022.02.009.
[21] M.E. Cinto, I.E. Dokmetzian, D.A. Ranalli, Iodophanus carneus and I. testaceus (Ascomycota-Pezizales): independent taxonomic identity or synonymy? A study of their morphology and isozymes, Bol. Soc. Argent. Bot 42 (2007) 181–187.
[22] A. Martinez-Gil, R. Caballero, Ascomicetos raros o interesantes de La Rioja,España (II), Bol. Micolog. FAMCAL 11 (2016) 73–88.
[23] Kosolapov A.I., Natural scientific methods in the examination of art works, State Herm, S.-Petersburg, 2015.
[24] A. Zhgun, D. Avdanina, K. Shumikhin, N. Simonenko, E. Lyubavskaya, I. Volkov, V. Ivanov, Detection of potential biodeterioration risks for tempera painting in 16th century exhibits from State Tretyakov Gallery, PLoS One 15 (2020) e0230591, doi:10.1371/journal.pone.0230591.
[25] L.A. Alexandrova, M.V. Jasko, S.D. Negrya, P.N. Solyev, O.V. Shevchenko, A.P. Solodinin, D.P. Kolonitskaya, I.L. Karpenko, O.V. Efremenkova, A.A. Glukhova, Y.V. Boykova, T.A. Efimenko, N.V. Kost, D.A. Avdanina, G.K. Nuraeva, I.A. Volkov, S.N. Kochetkov, A.A. Zhgun, Discovery of novel N4-alkylcytidines as promising antimicrobial agents, Eur. J. Med. Chem 215 (2021) 113212, doi:10.1016/j.ejmech.2021.113212.
[26] L.A. Alexandrova, I.A. Oskolsky, D.A. Makarov, M.V. Jasko, I.L. Karpenko, O.V. Efremenkova, B.F. Vasilyeva, D.A. Avdanina, A.A. Ermolyuk, E.E. Benko, S.G. Kalinin, T.V. Kolganova, M.Y. Berzina, I.D. Konstantinova, A.O. Chizhov, S.N. Kochetkov, A.A. Zhgun, New biocides based on N4-alkylcytidines: effects on microorganisms and application for the protection of cultural heritage objects of painting, Int. J. Mol. Sci. 25 (2024) 3053, doi:10.3390/IJMS25053053/S1.
[27] L.A. Alexandrova, O.V. Shevchenko, M.V. Jasko, P.N. Solyev, I.L. Karpenko, S.D. Negrya, O.V. Efremenkova, B.F. Vasilieva, T.A. Efimenko, D.A. Avdanina, G.K. Nuraeva, M.P. Potapov, V.I. Kukushkina, S.N. Kochetkov, A.A. Zhgun, 3′-Amino modifications enhance the antifungal properties of N4-alkyl-5-methylcytidines for potential biocides, New J. Chem. 46 (2022) 5614–5626, doi:10.1039/D1NJ04312A.
[28] E. Talik, Z. Plazek, 2-Chloro-3,5-dinitropyridine. I. Exchange reactions of the chlorine atom, Bull. l'Academie Pol. Des Sci. Ser. Des Sci. Chim 8 (1960) 219–222.
[29] A.M. Pesin, V.G. Khaletskii, Chemistry of 2,1,3-thia- and selenadiazoles. XIV. Reactivity of bromine in derivatives of benzo-2,1,3-thiadiazole, Zhurnal Obs. Khimii. 32 (1962) 3284–3290.
[30] V.A. Surovtsev, V.V. Makarov, Cyclic 5-nitropyridin-2-yl-thioalkenyl-4-dithiocarbamate derivatives having antifungal activity and use thereof, 2012. https://patents.google.com/patent/RU2487132C1/en..
[31] G. Degiacomi, L.R. Chiarelli, O. Riabova, N.I. Loré, L. Muñoz-Muñoz, D. Recchia, G. Stelitano, U. Postiglione, F. Saliu, A. Griego, V.C. Scoffone, E. Kazakova, E. Scarpa, J.M. Ezquerra-Aznárez, A. Stamilla, S. Buroni, E. Tortoli, L. Rizzello, D. Sassera, S. Ramón-García, D.M. Cirillo, V. Makarov, M.R. Pasca, The novel drug candidate VOMG kills mycobacterium abscessus and other pathogens by inhibiting cell division, Int. J. Antimicrob. Agents. 64 (2024), doi:10.1016/j.ijantimicag.2024.107278.
[32] E.K. Baylis, C.D. Campbell, J.G. Dingwall, 1-Aminoalkylphosphonous acids. Part 1. Isosteres of the protein amino acids, J. Chem. Soc. Perkin Trans. 1. (1984) 2845–2853, doi:10.1039/P19840002845.

[33] A.Y. Rudenko, S.S. Mariasina, A.K. Bolikhova, M.V. Nikulin, R.M. Ozhiganov, V.G. Vasil'ev, Y.A. Ikhalaynen, A.L. Khandazhinskaya, M.A. Khomutov, P.V. Sergiev, A.R. Khomutov, V.I. Polshakov, Organophosphorus S-adenosyl-L-methionine mimetics: synthesis, stability, and substrate properties, Front. Chem. 12 (2024), doi:10.3389/FCHEM.2024.1448747.
[34] A.R. Khomutov, T.I. Osipova, E.N. Khurs, K.V. Alferov, R.M. Khomutov, Synthesis of phosphinic and phosphonic analogs of aspartic acid, Russ. Chem. Bull. 45 (1996) 1961–1964, doi:10.1007/BF01457787/METRICS.
[35] T. Senphan, S. Benjakul, W. Sukketsiri, L. Chotphruethipong, C. Sriket, Comparative studies on characterizations and cytotoxicity of oil extracted from Lingzhi (Ganoderma lucidum) G2 spore using soxhlet extraction and microwave-assisted extraction, Appl. Food Res. 4 (2024), doi:10.1016/J.AFRES.2024.100483.
[36] T.G. Kudre, S.K. Bejjanki, B.W. Kanwate, P.Z. Sakhare, Comparative study on physicochemical and functional properties of egg powders from japanese quail and white leghorn chicken, Int. J. Food Prop. 21 (2018) 956–971, doi:10.1080/10942912.2018.1466320.
[37] N. Eastaugh, V. Walsh, C. T, S. R, Pigment Compendium—A Dictionary of Historical Pigments, Elsevier, Oxford, 2004.
[38] S. Kroustallis, M. Gómez González, M. Miquel Juan, R. Bruquetas Galán, O. Pérez Monzón, Gilding in Spanish panel painting from the fifteenth and early sixteenth centuries, J. Mediev. Iber. Stud. 8 (2016) 313–343, doi:10.1080/17546559.2016.1230273.
[39] H. Babich, G. Stotzky, Toxicity of zinc to fungi, bacteria, and coliphages: influence of chloride ions, Appl. Environ. Microbiol. 36 (1978) 906–914, doi:10.1128/AEM.36.6.906-914.1978.
[40] B. Klimek, M. Niklińska, Zinc and copper toxicity to soil bacteria and fungi from zinc polluted and unpolluted soils: a comparative study with different types of biolog plates, Bull. Environ. Contam. Toxicol. 78 (2007) 102–107, doi:10.1007/S00128-007-9045-6.
[41] G.D. Savi, A.J. Bortoluzzi, V.M. Scussel, Antifungal properties of zinc-compounds against toxigenic fungi and mycotoxin, Int. J. Food Sci. Technol. 48 (2013) 1834–1840, doi:10.1111/IJFS.12158.
[42] E. Caselli, S. Pancaldi, C. Baldisserotto, F. Petrucci, A. Impallaria, L. Volpe, M. D'Accolti, I. Soffritti, M. Coccagna, G. Sassu, F. Bevilacqua, A. Volta, M. Bisi, L. Lanzoni, S. Mazzacane, Characterization of biodegradation in a 17 th century easel painting and potential for a biological approach, PLoS One (2018) 13, doi:10.1371/JOURNAL.PONE.0207630.
[43] A.L. Khandazhinskaya, E.S. Matyugina, L.A. Alexandrova, V.A. Kezin, L.N. Chernousova, T.G. Smirnova, S.N. Andreevskaya, V.I. Popenko, O.G. Leonova, S.N. Kochetkov, Interaction of 5-substituted pyrimidine nucleoside analogues and M.Tuberculosis: a view through an electron microscope, Biochimie 171–172 (2020) 170–177, doi:10.1016/J.BIOCHI.2020.03.004.
[44] O.S. Ostroumova, S.S. Efimova, P.D. Zlodeeva, L.A. Alexandrova, D.A. Makarov, E.S. Matyugina, V.A. Sokhraneva, A.L. Khandazhinskaya, S.N. Kochetkov, Derivatives of pyrimidine nucleosides affect artificial membranes enriched with mycobacterial lipids, Pharmaceutics 16 (2024), doi:10.3390/PHARMACEUTICS16091110.
[45] G. Trespidi, V.C. Scoffone, G. Barbieri, F. Marchesini, A. Abualsha'ar, T. Coenye, F. Ungaro, V. Makarov, R. Migliavacca, E. De Rossi, S. Buroni, Antistaphylococcal activity of the ftsz inhibitor c109, Pathogens 10 (2021), doi:10.3390/PATHOGENS10070886.
[46] C.T. Supuran, Structure-based drug discovery of carbonic anhydrase inhibitors, J. Enzyme Inhib. Med. Chem. 27 (2012) 759–772, doi:10.3109/14756366.2012.672983.
[47] R. McKenna, C.T. Supuran, Carbonic anhydrase inhibitors drug design, Subcell. Biochem 75 (2014) 291–323, doi:10.1007/978-94-007-7359-2_15.
[48] V. M, E.G. Salina, S. Huszár, J. Zemanová, J. Keruchenko, O. Riabova, E. Kazakova, A. Grigorov, T. Azhikina, A. Kaprelyants, K. Mikušová, Copper-related toxicity in replicating and dormant mycobacterium tuberculosis caused by 1-hydroxy-5-R-pyridine-2(1H)-thiones, Metallomics 10 (2018) 992–1002, doi:10.1039/c8mt00067k.
[49] R.M. Khurs, E.N. Osipova, T.I. Khomutov, Enzyme reamination of phosphororganic analogs of aspartate and glutamate, Bioorg. Khim. 15 (1989) 552–555.
[50] T. McFate, A. Mohyeldin, H. Lu, J. Thakar, J. Henriques, N.D. Halim, H. Wu, M.J. Schell, M.T. Tsz, O. Teahan, S. Zhou, J.A. Califano, H.J. Nam, R.A. Harris, A. Verma, Pyruvate dehydrogenase complex activity controls metabolic and malignant phenotype in cancer cells, J. Biol. Chem. 283 (2008) 22700–22708, doi:10.1074/jbc.M801765200.
[51] K.S. Ju, J. Gao, J.R. Doroghazi, K.K.A. Wang, C.J. Thibodeaux, S. Li, E. Metzger, J. Fudala, J. Su, J.K. Zhang, J. Lee, J.P. Cioni, B.S. Evans, R. Hirota, D.P. Labeda, W.A. Van Der Donk, W.W. Metcalf, Discovery of phosphonic acid natural products by mining the genomes of 10,000 actinomycetes, Proc. Natl. Acad. Sci. U. S. A. 112 (2015) 12175–12180, doi:10.1073/PNAS.1500873112.
[52] V.L. Filonov, M.A. Khomutov, A.V. Sergeev, A.L. Khandazhinskaya, S.N. Kochetkov, E.S. Gromova, A.R. Khomutov, Interaction of DNA methyltransferase Dnmt3a with phosphorus analogues of S-adenosylmethionine and S-adenosylhomocysteine, Mol. Biol. (Mosk). 57 (2023) 717–725, doi:10.31857/S0026898423040079.
[53] Y.N. Zhukov, N.A. Vavilova, T.I. Osipova, T.M. Voinova, E.N. Khurs, V.G. Dzhavakhia, R.M. Khomutov, Fungicidal activity of phosphinic analogues of amino acids involved in methionine metabolism, Dokl. Biochem. Biophys. 397 (2004) 210–212, doi:10.1023/B:DOBI.0000039465.65071.6E.
[54] Y.N. Zhukov, N.A. Vavilova, T.I. Osipova, E.N. Khurs, V.G. Dzhavakhiya, R.M. Khomutov, New synthesis and fungicidal activity of the phosphine analogues of serine and threonine, Mendeleev Commun 15 (2005) 57–58, doi:10.1070/MC2005V015N02ABEH001940.
[55] Y.N. Zhukov, N.A. Vavilova, T.I. Osipova, E.N. Khurs, V.G. Dzhavakhiya, R.M. Khomutov, New synthesis and fungicidal activity of a phosphinic analogue of glycine, Mendeleev Commun 14 (2004) 93, doi:10.1070/MC2004V014N03ABEH001864.
[56] Y.N. Zhukov, N.A. Vavilova, T.I. Osipova, T.M. Voinova, E.N. Khurs, V.G. Dzhavakhiya, R.M. Khomutov, Aminoalkylphosphinates are new effective inhibitors of melanogenesis and fungicides, Dokl. Biochem. Biophys. 398 (2004) 304–306, doi:10.1023/B:DOBI.0000046644.42683.0F.
[57] Z.T. Schug, B. Peck, D.T. Jones, Q. Zhang, S. Grosskurth, I.S. Alam, L.M. Goodwin, E. Smethurst, S. Mason, K. Blyth, L. McGarry, D. James, E. Shanks, G. Kalna, R.E. Saunders, M. Jiang, M. Howell, F. Lassailly, M.Z. Thin, B. Spencer-Dene, G. Stamp, N.J.F. van den Broek, G. Mackay, V. Bulusu, J.J. Kamphorst, S. Tardito, D. Strachan, A.L. Harris, E.O. Aboagye, S.E. Critchlow, M.J.O. Wakelam, A. Schulze, E. Gottlieb, Acetyl-CoA synthetase 2 promotes acetate utilization and maintains cancer cell growth under metabolic stress, Cancer Cell 27 (2015) 57–71, doi:10.1016/j.ccell.2014.12.002.
[58] R.M. Khomutov, I.N. Zhukov, A.R. Khomutov, E.N. Khurs, D.L. Kramer, J.T. Miller, C.W. Porter, Phosphinic analog of methionine inhibits growth of leucosis cell L1210 and transforms to phosphinic analog of S-adenosylmethionine, Bioorg. Khim. 26 (2000) 718–720.